ELSEVIER

Polymer 42 (2001) 5365–5370

polymer

www.elsevier.nl/locate/polymer

Application of the Ozawa model to non-isothermal crystallization of poly(ethylene terephthalate)

P. Sajkiewicz[a,*], L. Carpaneto[b], A. Wasiak[a]

[a]*Polish Academy of Sciences, Institute of Fundamental Technological Research Swiętokrzyska 21, 00-049 Warsaw, Poland*
[b]*Genoa University, Department of Chemistry, Via Dodecaneso 31, 16-146 Genova, Italy*

Received 5 March 1999; received in revised form 20 November 2000; accepted 5 December 2000

Abstract

The non-isothermal crystallization of poly(ethylene terephthalate) (PET) during cooling with constant rates is investigated by differential scanning calorimetry (DSC). The analysis is aided by microscopic investigation of the final morphology. The results are analyzed using the Ozawa model. It is shown that this model describes the non-isothermal process only at relatively low cooling rates. At rates exceeding 20°/min, crystallization progress becomes higher, indicating higher crystallization rates than those resulting from the Ozawa approach. Additional deviation from the Ozawa model observed at the very beginning and the end of crystallization can be attributed to spatial constraints of spherulitic growth. In the first case, the spherulitic growth is impeded by the dense instantaneous nucleation on the polymer surface (transcrystallization) and in the second one by impingements of bulk growing spherulites.

Keywords: Non-isothermal crystallization; Ozawa model; Poly(ethylene terephthalate)

1. Introduction

For long, the non-isothermal crystallization of polymers has been investigated by many researchers. Although the process of non-isothermal crystallization of slowly crystallizing materials, like polymers, is probably relatively complex, it is very attractive to describe it using rather simple models. One of the methods commonly applied for the analysis of non-isothermal crystallization kinetic data was proposed by Ozawa [1]. He assumed that the process of non-isothermal crystallization is governed by the same mechanism as that predicted by Kolmogorov [2], Avrami [3,4] and Evans [5] (KAE model) for the process of isothermal crystallization for which

$$1 - x_{\mathrm{rel}} = \exp[-k(T)t^n] \tag{1}$$

where x_{rel} is the relative crystallinity, $k(T)$ is the crystallization rate, and n is the Avrami exponent. Eq. (1) is often written in a somewhat different form:

$$1 - x_{\mathrm{rel}} = \exp[-K(T)t]^n \tag{2}$$

where

$$K = k^{1/n} \tag{2a}$$

In a non-isothermal process there is a change of temperature with time, leading to the dependence of the crystallization rate on time. The Ozawa equation for constant rate of temperature changes, $(\mathrm{d}T/\mathrm{d}t) = \mathrm{const}$, is given by [1]:

$$1 - x_{\mathrm{rel}} = \exp\left(\frac{-\kappa(T)}{|\mathrm{d}T/\mathrm{d}t|^n}\right) \tag{3}$$

where $\kappa(T)$ is the so-called cooling function of non-isothermal crystallization. Taking the logarithm of Eq. (3) twice yields

$$\ln[-\ln(1 - x_{\mathrm{rel}})] = \ln[\kappa(T)] + n\ln\left(\frac{1}{|\mathrm{d}T/\mathrm{d}t|}\right) \tag{4}$$

If the Ozawa approach is valid the plot of $\ln[-\ln(1 - x_{\mathrm{rel}})]$ versus $\ln|(\mathrm{d}T/\mathrm{d}t)^{-1}|$ for constant temperatures should be linear with n as the slope and $\kappa(T)$ as the intercept. So far, the Ozawa model has been successfully used for the description of the non-isothermal crystallization of poly(ethylene terephthalate) (PET) [1], polypropylene [6–8], polyamide 6 [9] poly(*p*-phenylene sulphide) [10], and new TPI [11]. On the other hand, the non-linearity of the Ozawa plot was observed in the case of polyethylene [6], PEEK [12], PEEKK [13] and poly(arylene ether ether sulfide) [14]. It

* Corresponding author. Tel.: +48-22-8261281, ext. 148; fax: +48-22-8269815.

E-mail addresses: psajk@ippt.gov.pl (P. Sajkiewicz), carpanet@unige.it (L. Carpaneto), awasiak@ippt.gov.pl (A. Wasiak).

0032-3861/01/$ - see front matter
PII: S0032-3861(00)00934-4

is worth stressing that both the Ozawa and KAE models are included in the Nakamura equation [15,16]:

$$1 - x_{rel} = \exp\left\{-\left[\int_0^t K(T)\,dt\right]^n\right\} \quad (5)$$

For isothermal conditions, Eq. (5) reduces directly to the Avrami equation since for isothermal processes the isokinetic models do not consider the time dependence of crystallization rate.

In the non-isothermal case with constant rate of change of temperature (dT/dt) = const, Eq. (5) can be reformulated as a function of T and reduces to Ozawa equation (3) with

$$\left[\int_{T(0)}^{T(t)} K(T)\,dT\right]^n = \kappa(T) \quad (6)$$

integrated between temperatures $T(0)$ and $T(t)$.

It was shown by Hieber [17] that it is possible to find the relation between the Avrami and Ozawa parameters using the Nakamura equation. A similar relation was derived by Wasiak [18]. Eq. (6) can be rewritten as

$$\int_{T(0)}^{T(t)} K(T)\,dT = [\kappa(T)]^{1/n} \quad (7)$$

Differentiation of Eq. (7) with respect to T (lower boundary) allow the determination of the crystallization rate K

$$K = -d[(\kappa(T))^{1/n}]/dT \quad (8)$$

from the known value of the Ozawa cooling function κ found for non-isothermal crystallization.

This paper discusses the application of the Ozawa model to the non-isothermal crystallization of PET analyzed within a broad range of cooling rates. The analysis is aided by the microscopic investigation of the morphology, which allows us to separate the effect of the exponent n on the Ozawa plots.

2. Experimental

2.1. Material

Commercial PET, fiber spinning grade ($M_w = 40.4 \times 10^3$ and $M_n = 22.5 \times 10^3$) made by ICI was investigated. Before experiments, the polymer was dried under vacuum at 150°C for 12 h.

2.2. Method

2.2.1. Differential scanning calorimetry (DSC)

Crystallization was carried out using the differential scanning calorimeter model Perkin–Elmer DSC-7 calibrated with indium during heating at the rate of 10°/min. During the experiment, the polymer was purged with nitrogen. The weight of the samples ranged from 13 to 16 mg. Crystallization was preceded by heating of the sample to 290°C and holding it in the molten state at 290°C for 10 min.

2.2.2. Non-isothermal crystallization

Non-isothermal crystallization was performed during cooling with constant rates being in the range between 1 and 90°/min. The temperature was additionally corrected for the temperature gradient between the sample and the furnace according to the method proposed by Janeschitz-Kriegl et al. [19,20]. It is known that in non-isothermal conditions there is a temperature lag between the sample and furnace. The applied correction considered both components of the temperature gradient, e.g. the temperature difference between the furnace and the bottom of the pan as well as that existing inside a sample. The temperature of the furnace, $T_f(t)$, is converted into internal temperature in the sample, $T(t)$, using the equation [20]

$$T(t) = T_f(t) - \frac{dT/dt}{\alpha} + \frac{\Phi(t)}{\gamma} \quad (9)$$

where dT/dt is the applied rate of temperature changes, Φ the heating power, and γ an effective heat transfer coefficient given by

$$\gamma = \alpha(m_p c_p + m_s c_s) \quad (10)$$

where m_p and m_s are the masses of the pan and the sample, c_p and c_s the corresponding heat capacities, and α the coefficient determined directly from the experiment as a slope of the plot of $|dT/dt|\ln(\Phi(T_f))$ versus T_f in the range after the maximum of the signal. According to Refs. [19,20] it is expected that the plot of $|dT/dt|\ln(\Phi(T_f))$ versus T_f in the range after the maximum of the signal should be linear with the slope independent of cooling rate. Our results indicate that the linearity of this plot is rather questionable. The comparison of those plots at various cooling rates shows that the value of 0.16 (s^{-1}) as determined in Ref. [20] for PP can be found only at high cooling rates at the end of the crystallization peak. We suppose that the difficulties in the determination of α might be due to a few reasons. The most important is related to the fact that the pans used by us were standard pans with a slightly bent bottom as a consequence of the closing procedure, while those applied in Refs. [19,20] were specially modified in order to have the same contact between the bottom of the pan and the flat DSC support in each experiment. The second reason could be related to the nature of PET crystallization. Putting $\alpha =$ 0.16 and heat capacities at 200°C of aluminum $c_p =$ 0.993J K^{-1} g^{-1} and PET $c_s = 1.93$ J K^{-1} g^{-1} [21] results in γ in the range between 8.3 and 9.2 mW K^{-1} for sample masses between 13 and 16 mg and pan weight of 27 mg. Considering the narrow range of sample masses, we decided to use $\alpha = 0.16$ and $\gamma = 9$ mW K^{-1} for temperature correction.

Relative crystallinity, x_{rel}, was determined from DSC thermograms using the equation

$$x_{rel} = \frac{\int_{T(0)}^{T(t)} \left(\frac{dQ}{dt}/\frac{dT}{dt}\right) dT}{\int_{T(0)}^{T_\infty} \left(\frac{dQ}{dt}/\frac{dT}{dt}\right) dT} \quad (11)$$

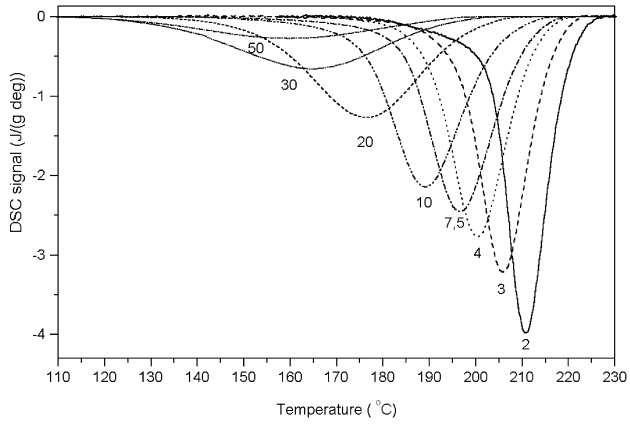

Fig. 1. DSC thermograms for various cooling rates. Cooling rates in degrees per minute indicated.

where (dQ/dt) is the rate of evolution of crystallization heat, which after dividing by cooling rate, (dT/dt), is integrated in the range from the temperature $T(0)$, at which crystallization starts, to the actual temperature $T(t)$ and to the end temperature of crystallization T_∞. In addition, absolute crystallinity was computed using the value of enthalpy difference per unit mass between the amorphous and the completely crystalline polymer equal to 140 J g^{-1} [22].

The Avrami exponent n and the cooling function κ for non-isothermal crystallization were determined as a slope and intercept of the plot of $\ln[-\ln(1-x_{rel})]$ versus $\ln\left|(dT/dt)^{-1}\right|$ for constant temperatures. The Avrami crystallization rate K was determined using Eq. (8). In order to assess an experimental error, DSC runs at some cooling rates were repeated several times.

2.2.3. Optical investigations

After cooling to room temperature, the samples were removed from calorimetric pans, cut into thin slices with an ultramicrotome and observed between crossed polarizers using transmission polarization–interference microscope MPI 5 produced by Polish Optical Works (PZO).

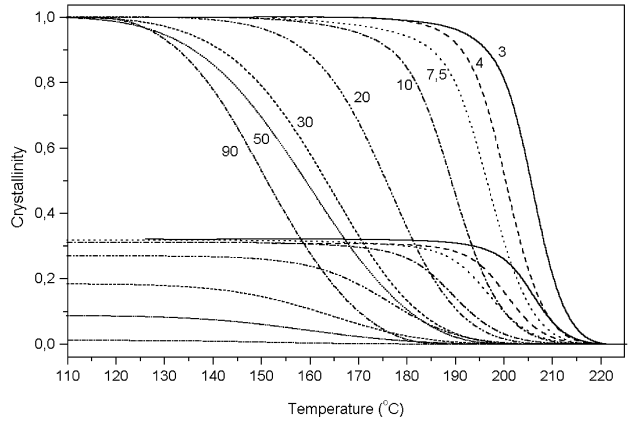

Fig. 2. Relative and absolute crystallinity from DSC thermograms versus temperature for various cooling rates (indicated).

3. Results and discussion

Fig. 1 illustrates typical DSC thermograms and Fig. 2 the progress of crystallization during cooling at various rates. It is seen that the earlier crystallization starts, the lower the cooling rate. Absolute crystallinity at the end of crystallization decreases with cooling rate.

Fig. 3 shows experimental data plotted in Ozawa coordinates. It is seen that the Ozawa plot deviates from linear at the beginning and at the end of crystallization. Independent information concerning the morphology, which is obtained directly from optical investigations, allows us to distinguish between the effect of the geometry of growing crystallites alone and other possible reasons for the non-linearity of the Ozawa plot. The analysis of the morphology formed during non-isothermal crystallization (Fig. 4) clearly shows that in addition to bulk nucleated spherulites, there is a narrow zone of transcrystallinity on the top and bottom surface of the polymer. This is the result of very dense nucleation on the polymer surface, leading to practically unidirectional growth perpendicular to the polymer surface. A similar process of transcrystallization during the cooling of polyamide 6-6 was observed by Billon et al. [23,24]. In our opinion, such a dense nucleation on the polymer surfaces can be a heterogeneous process occurring on impurities collected on the polymer surface. This hypothesis is supported by the observation that when a DSC sample was prepared by putting a few pieces of polymer into a pan, the lines of dense nucleation were observed not only on the top and bottom surfaces but also inside the polymer (Fig. 4e). The evidence that the observed transcrystallinity appears at the beginning of non-isothermal crystallization can be deduced from the observation that transcrystallinity forms the continuous layer without any interruption by the bulk nucleated spherulites. Transcrystallization is a process of growth with spatial constraints leading to a value of exponent n different from that for three-dimensional growth

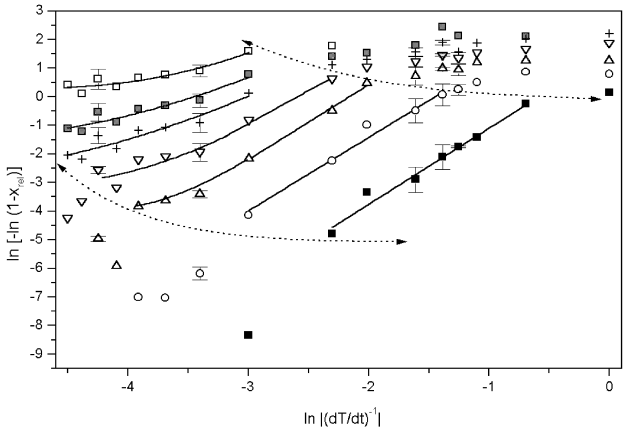

Fig. 3. Ozawa plot for non-isothermal crystallization at different temperatures: (□) 140, (●) 160, (+) 170, (▽) 180, (△) 190, (○) 200, and (■) 210°C. The data between broken lines fulfill the conditions of unconstrained growth. The mean error of the mean values is shown for some cooling rates.

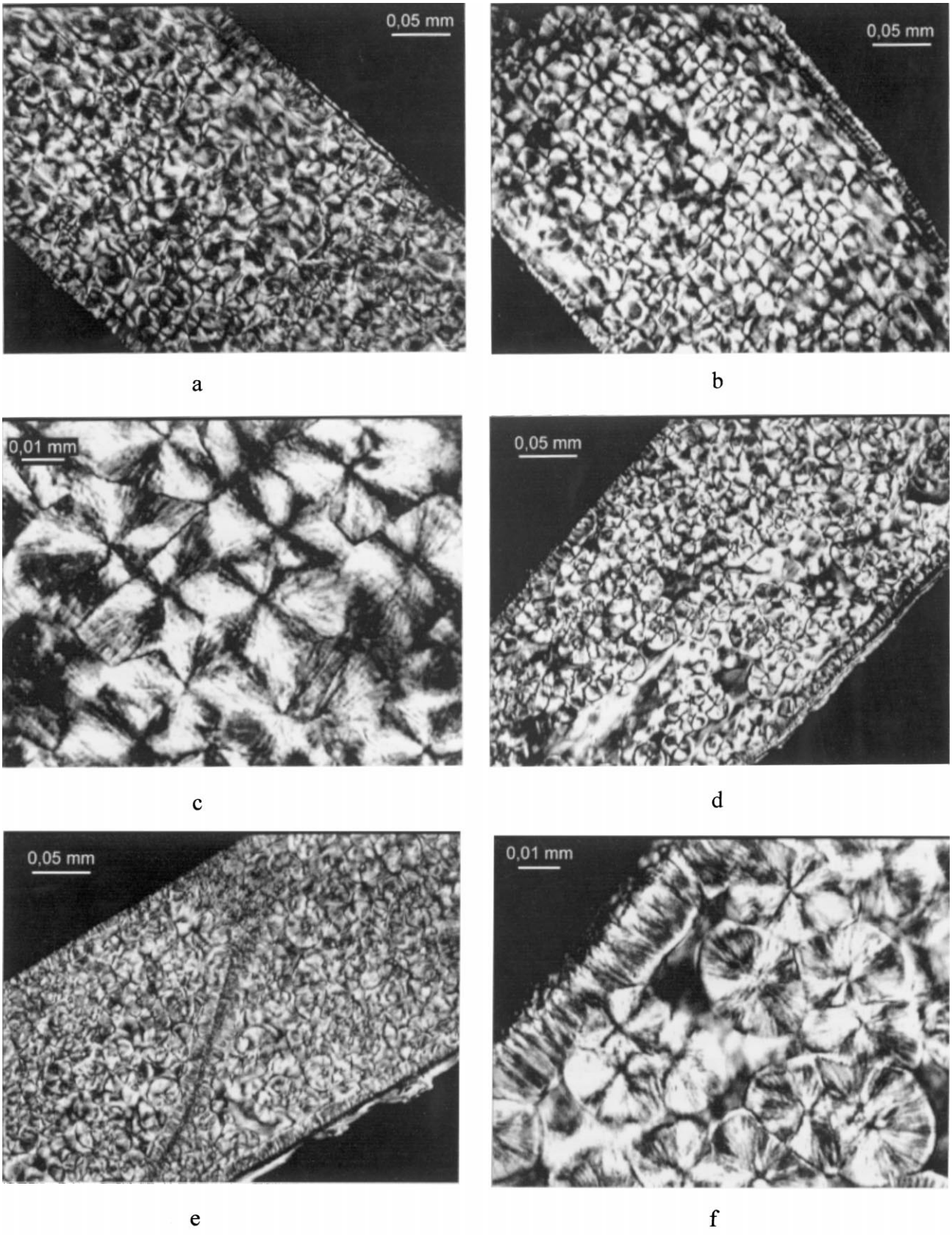

Fig. 4. Micrographs taken from the samples after crystallization in DSC with various cooling rates (°/min): (a) 6, (b) 10, (c) 10, (d) 20, (e) 20, (f) 20, (g) 40, and (h) 50. Cutting plane perpendicular to the bottom of DSC pans.

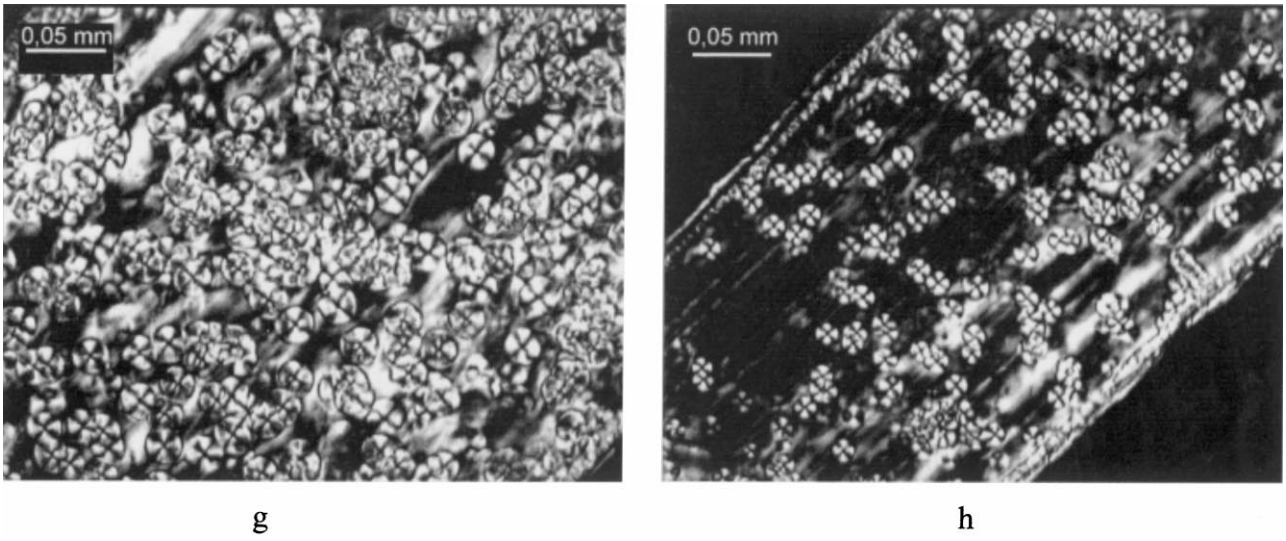

Fig. 4. (*continued*)

assumed in the KAE model. If the observed transcrystallites are indeed heterogeneously nucleated, it should lead to additional changes of the exponent n. In order to estimate the range of crystallinity within which the non-linearity of the Ozawa plot is caused by the deviation of the exponent n from that for three-dimensional growth, it is necessary to assess the content of transcrystalline morphology. We did not observed any effect of cooling rate on the thickness of the transcrystalline layer. We estimate that the final content of the transcrystalline layer with respect to the volume of a sample is to the order of a few percent. In terms of the absolute crystallinity, the content of the transcrystalline zone increases with cooling rate since the fraction of bulk nucleated spherulites decreases. The lower broken line in Fig. 3 is the limit below which, according to our results, deviation from the linearity of the Ozawa plot is caused by spatial constraints during the growth of the crystallites. A similar process of spatial constraint during growth is responsible for the deviation of the Ozawa plot at the end of crystallization (data above the upper broken line in Fig. 3). The impingement of bulk nucleated spherulites with neighbors at the end of crystallization is an obvious and well-documented process. The relative crystallinity at which impingement becomes essential increases with cooling rate. This is due to the fact that an increase of cooling rate causes a decrease of absolute crystallinity, and therefore an increase of the fraction of amorphous phase between spherulites (Fig. 4). At cooling rates higher than 40°/min, at which a large amount of amorphous phase between spherulites remains after crystallization (Fig. 4g and h), the effect of truncation can be neglected.

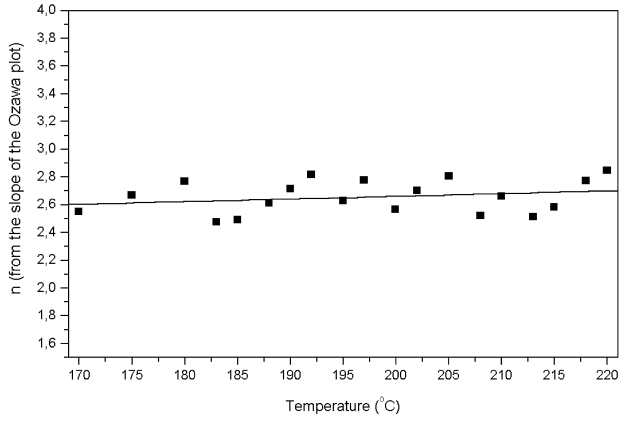

Fig. 5. The exponent n determined from the linear part of the Ozawa plot versus temperature.

The analysis of the data within the range of unimpeded spherulitic growth (data between the broken lines in Fig. 3) shows that there is still deviation of the Ozawa plot from linear dependence at cooling rates above 20°/min. The linear function as predicted by Ozawa is observed only for data obtained at relatively low cooling rates. The curvature of the non-linear parts of the Ozawa plots in Fig. 3 is positive, indicating that at high cooling rates, at any instant of time, the crystallinity is higher than it is resulting from the Ozawa model. When the data are not corrected for the temperature gradient, the non-linearity of the Ozawa plot is slightly weaker; however, it is still observed. Considering that the exponent n is constant within this range of crystallization, the presented data indicate that the reason for this non-linearity is related to the higher crystallization rate at high cooling rates than that resulting from the isokinetic Ozawa model. The interpretation of such behavior can be made on the basis of the new model recently proposed by Ziabicki [25–27]. He takes into account two mechanisms, athermal and relaxational, leading to the direct dependence of crystallization rate on time in addition to those resulting from the change of temperature. Ziabicki's crystallization rate should be different from the isokinetic value resulting from the Ozawa model. According to Ziabicki [25–27] this

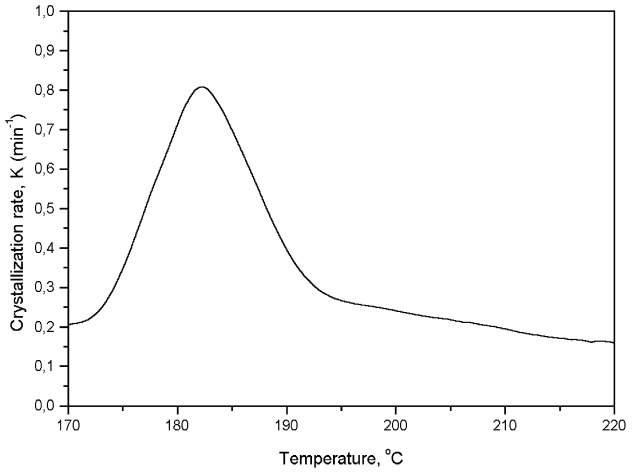

Fig. 6. Crystallization rate K versus temperature determined from non-isothermal data using the Ozawa model. Approximation with Pearson VII function.

difference should increase with the rate of temperature changes. In the next paper we will discuss the kinetic data using the Ziabicki approach.

It is possible to determine the Avrami exponent and the cooling function κ from a slope and intercept, respectively, of the linear portion of the Ozawa plots (Eq. (4)) and hence find the Avrami crystallization rate, K (Eq. (8)). It is seen in Fig. 5 that the Avrami exponent is practically independent of temperature over the temperature range available (170–220°C). The standard deviation of the experimental data from the linear approximation seen in Fig. 5 is 0.12 and the temperature averaged value of n is 2.65. The value of the exponent n close to 3 describes either the process of instantaneous nucleated three-dimensional growth or sporadic nucleated two-dimensional growth. The plot of crystallization rate, K, as a function of temperature, was determined from the Ozawa cooling function approximated with the function of sigmoidal shape given by the Boltzmann equation. The resulting crystallization rate, K, plotted in Fig. 6, was determined with $n = 2.65$. It is seen in Fig. 6 that the maximum crystallization rate occurs at 182.5°C.

References

[1] Ozawa T. Polymer 1971;12:150.
[2] Kolmogorov N. Izv Akad Nauk USSR Ser Math 1937;1:355.
[3] Avrami M. J Phys Chem 1939;7:1103.
[4] Avrami M. J Phys Chem 1941;9:177.
[5] Evans UR. Trans Faraday Soc 1945;41:365.
[6] Eder M, Włochowicz A. Polymer 1983;24:1593.
[7] Hammami A, Spruiell JE. Polym Engng Sci 1995;35:797.
[8] Monasse B, Haudin JM. Colloid Polym Sci 1986;264:117.
[9] Kozłowski W. J Polym Sci (C) 1972;38:47.
[10] Lopez LC, Wilkes GL. Polymer 1989;30:882.
[11] Friler JB, Cebe P. Polym Engng Sci 1993;33:587.
[12] Cebe P, Hong SD. Polymer 1986;27:1183.
[13] Liu T, Mo Z, Wang S, Zhang H. Polym Engng Sci 1997;37:568.
[14] Srivinas S, Babu JR, Riffle JS, Wilkes GL. Polym Engng Sci 1997;37:497.
[15] Nakamura K, Watanabe T, Katayama K, Amano T. J Appl Polym Sci 1972;16:1077.
[16] Nakamura K, Watanabe T, Katayama K, Amano T. J Appl Polym Sci 1973;17:1031.
[17] Hieber CA. Polymer 1995;36:1455.
[18] Wasiak A. Chemtracts — Macromol Chem 1991;2:211.
[19] Janeschitz-Kriegl H, Wippel H, Paulik Ch, Eder G. Colloid Polym Sci 1993;271:1107.
[20] Eder G, Janeschitz-Kriegl H. Crystallization. In: Meijer HEH, editor. Processing of polymers, Materials science and technology, vol. 18. Weinheim: VCH, 1997 (chap. 5).
[21] Mark JE, editor. Physical properties of polymers, handbook. Woodbury, NY: American Institute of Physics, 1996.
[22] Wunderlich B. Crystal melting, Macromolecular physics, vol. 3. New York: Academic Press, 1980.
[23] Billon N, Magnet C, Haudin JM, Lefebvre D. Colloid Polym Sci 1994;272:633.
[24] Billon N, Magnet C, Haudin JM. Proceedings of PPS Conference, New Delhi, 1992. 186pp.
[25] Ziabicki A. Colloid Polym Sci 1996;274:209.
[26] Ziabicki A. Colloid Polym Sci 1996;274:705.
[27] Ziabicki A, Sajkiewicz P. Colloid Polym Sci 1998;276:680.